Hyperfine Interactions manuscript No.
(will be inserted by the editor)

Atomic parity non-conservation: the francium anapole project of the FrPNC collaboration at TRIUMF

S. Aubin · J. A. Behr · R. Collister · V. V. Flambaum · E. Gomez · G. Gwinner · K. P. Jackson · D. Melconian · L. A. Orozco · M. R. Pearson · D. Sheng · G. D. Sprouse · M. Tandecki · J. Zhang · Y. Zhao

Received: date / Accepted: date

S. Aubin
Dept. Physics, College of William and Mary, Williamsburg, VA 23197, USA.

J. A. Behr, K. P. Jackson, M. R. Pearson, M. Tandecki
TRIUMF, Vancouver, BC V6T 2A3, Canada.

V. V. Flambaum
School of Physics, University of New South Wales, Sydney 2052, Australia.

E. Gomez
Instituto de Fisica, Universidad Autonoma de San Luis Potosi, San Luis Potosi 78000, Mexico.

G. Gwinner, R. Collister, M. Tandecki
Dept. of Physics and Astronomy, University of Manitoba, Winnipeg, , MB R3T 2N2, Canada.

D. Melconian
Cyclotron Institute, Texas A&M University, College Station, TX 77843, USA.

L. A. Orozco E-mail: lorozco@umd.edu, D. Sheng, J. Zhang
JQI, Dept. of Physics, and NIST, University of Maryland, College Park, MD 20742, USA.
Present address: of D. Sheng Princeton University, Princeton, NJ 08544, USA.

G. D. Sprouse
Dept. of Physics and Astronomy, Stony Brook University, Stony Brook, NY 11794, USA.

Y. Zhao
State Key Laboratory of Quantum Optics and Quantum Optics Devices, Shanxi University, Taijuan 030006, China.

Abstract We present a method for measuring the nuclear anapole in a string of francium isotopes. The anapole is a parity non-conserving electromagnetic moment that enables parity-forbidden transitions between ground state hyperfine levels of an atom. The experiment is run by the FrPNC collaboration and relies on a beam of artificially-produced francium from the ISAC facility at TRIUMF.

Keywords atomic parity non-conservation · francium · weak interactions

PACS 31.30.jg · 12.15-y · 31.30.Gs

1 Introduction

Parity non-conservation (PNC) is a unique signature of the weak interaction. The weak interaction mixes states of opposite parity and produces two types of PNC effects in atoms: nuclear spin independent (*nsi*) and nuclear spin dependent (*nsd*) [1]. While our FrPNC collaboration is working on measurements of both types of PNC effects, this contribution focuses on the second [2]. Nuclear spin dependent PNC occurs in three ways [3,4]: (i) an electron interacts weakly with a single valence nucleon (nucleon axial-vector current and electron vector currents A_nV_e), (ii) an electron experiences an electromagnetic interaction with a nuclear chiral current created by parity-violating weak interactions between nucleons (anapole moment) [4,5], and (iii) the combined action of the hyperfine interaction and the spin-independent Z^0 exchange interaction from nucleon vector currents (V_nA_e) [6–8].

All recent and on-going experiments in atomic PNC rely on the large enhancement of the effect in heavy nuclei (large Z), first pointed out by the Bouchiats [9–11]. The attractiveness of Fr, the heaviest alkali atom, for atomic parity nonconservation (APNC) experiments has been discussed since the early 1990s in the context of searches for new physics beyond the Standard Model (SM) [12–15]. The atomic theory and structure of Fr can be understood at a level similar to that of Cs (Z = 55), where the most precise measurement to date has been performed, yet the APNC measurable effect is 18 times larger [16,17].

The weak interaction transition amplitudes are exceedingly small, and an interference method is commonly used to measure them. A typical experiment measures a quantity that has the form

$$|A_{\rm PC} + A_{\rm PNC}|^2 = |A_{\rm PC}|^2 + 2Re(A_{\rm PC}A^*_{\rm PNC}) + |A_{\rm PNC}|^2, \qquad (1)$$

where $A_{\rm PC}$ and $A_{\rm PNC}$ represent the parity conserving and parity non-conserving amplitudes. The second term on the right side corresponds to the interference term and can be isolated because it changes sign under a parity transformation. All experiments rely on atomic calculations to extract weak interaction parameters, so a high precision understanding of the electronic structure is crucial for APNC-based tests of nuclear theory and the standard model.

The current and recent APNC experiments follow two main strategies (see the review by the Bouchiats [18]). The first one is optical activity in an atomic vapor. The method has been applied to reach a precision of 2% in Bi[19], 1.2% in Pb [20,21], and 1.2% in Tl including the extraction also a limit for the anapole moment [22]. These three atoms present difficulties to the atomic theory and extraction of weak interaction parameters is less accurate than in Cs.

The second strategy measures the excitation rate of a highly forbidden transition. The electric dipole transition between the $6s$ and $7s$ levels in Cs becomes allowed through the weak interaction. Interference between this transition and the one induced by the Stark effect due to the presence of an static electric field generates a signal proportional to the weak charge. The best atomic PNC measurement to date uses this method to reach a precision of 0.35% [23,24] on the *nsi*-APNC. They measured the signal among different hyperfine levels and extracted the *nsd*-APNC contribution with an accuracy of 14% giving the first definite measurement of an anapole moment [6].

Other methods have also been proposed and pursued. The following are examples and do not intend to cover all the developments in the field: The Bouchiat group in Paris worked on the highly forbidden $6s$ to $7s$ electric dipole transition in a cesium cell, but detected the occurrence of the transition using stimulated emission rather than fluorescence [25]. The Budker group in Berkeley has completed a first round of measurements in ytterbium [26–29], has proposed APNC measurements with two-photon transitions [30], and is pursuing dysprosium [31,32]. There is an on-going experiment in the Blinov and Fortson group in Seattle using a single barium ion [33–35]. The Jungmann group at KVI is pursuing an APNC measurement in a single radium ion [36]. Significant process has occurred in atomic calculations for all these atoms. The DeMille group at Yale is working towards a direct anapole measurement with molecules [37].

2 Principle of the anapole measurement in Fr

Experimentally we can only measure the sum of the three terms that contribute to *nsd*-APNC. In heavy atoms, the anapole moment dominates the other two processes. For example, in ^{209}Fr the anapole part is a factor of 15 larger than the other two [5]. The other two mechanisms, which can be theoretically calculated from precise Standard Model predictions, can then be subtracted from the measured quantity to isolate the anapole moment part.

There are two general ways to experimentally measure the *nsd*-PNC signal. The first one measures the total (optical) APNC signal for appropriate combinations of hyperfine states better than 1%. The average gives the *nsi*-APNC and the difference the *nsd*-APNC one. Both of the finished experiments that bounded or measured an anapole moment in atomic physics used this method [22,23].

We propose to use a different method to directly measure the nuclear anapole moment by driving an electromagnetically forbidden electric dipole ($E1$) transition between the two ground hyperfine states with a field $\mathbf{E}_{E1}$. We denote the two states involved as $|s, F_i\rangle$, the *nsi*-PNC coupling coefficients as $\epsilon_{\rm nsi}$, and the *nsd*-PNC coupling coefficients as $\epsilon_{\rm nsd}(F_i)$. The modified states in the presence of the weak interaction are:

$$\begin{aligned}|s, \widetilde{F_1, m_{F_1}}\rangle &= |s, F_1, m_{F_1}\rangle + i\epsilon_{\rm nsi}|p, F_1, m_{F_1}\rangle + i\epsilon_{\rm nsd}(F_1)|p, F_1, m_{F_1}\rangle \\ |s, \widetilde{F_2, m_{F_2}}\rangle &= |s, F_2, m_{F_2}\rangle + i\epsilon_{\rm nsi}|p, F_2, m_{F_2}\rangle + i\epsilon_{\rm nsd}(F_2)|p, F_2, m_{F_2}\rangle, \quad (2)\end{aligned}$$

where the imaginary factor i is for the conservation of time reversal symmetry, assuming that $\epsilon_{\rm nsi}$ and $\epsilon_{\rm nsd}$ are real. The coupled p state has the same J value as the s state, which is $J = 1/2$. This leads to:

$$\langle s, \widetilde{F_2, m_{F_2}}|\mathbf{d}|s, \widetilde{F_1, m_{F_1}}\rangle = i(\epsilon_{\rm nsd}(F_1) - \epsilon_{\rm nsd}(F_2))\langle p, F_2, m_{F_2}|\mathbf{d}|s, F_1, m_{F_1}\rangle. \quad (3)$$

For ^{209}Fr, $\epsilon_{\rm nsd}(F) = -5.9 \times 10^{-13}\kappa_a[F(F+1) - 22.5]$ [38].

The lifetime of the states does not limit the coherent interaction time, because for all practical purposes, the spontaneous decay from the upper to the lower ground state of the hyperfine splitting can be neglected. Unfortunately, the parity-violating transition amplitude (A_{PNC}) is much too small to observe directly, so we need to amplify the signal by interfering it (see Eq. 1) with a coherent and much stronger parity-conserving transition amplitude (A_{PC}) between the same two states. In our case we add an auxiliary microwave field $\mathbf{B}_{M1}$ propagating parallel to an external DC magnetic field $\mathbf{B}_{DC}$ that drives the allowed $M1$ transition and induces Rabi oscillations between the two hyperfine states [39]. The directions (polarization) of the three fields: $\mathbf{E}_{E1}$, $\mathbf{B}_{M1}$ and $\mathbf{B}_{DC}$ define the handedness and the relevant pseudoscalar of the experiment $i\mathbf{E}_{E1} \times \mathbf{B}_{M1} \cdot \mathbf{B}_{DC}$.

If we start with N atoms in $|1\rangle$, the number of atoms ending up in $|2\rangle$ after an interaction time t_c is:

$$N_2 = N \sin^2\left(\frac{\sqrt{A_{\rm PC}^2 + A_{\rm PNC}^2 + 2A_{\rm PC}A_{\rm PNC}\cos\phi}\, t_c}{2\hbar}\right), \quad (4)$$

where ϕ is the relative phase difference between these two transitions. By tuning these two transitions in phase and π out of phase, we have a maximum change in the interference term. This change of π in the relative phase relation is effectively equivalent to the reversal of the handedness of the experimental coordinate system. The signal comes from the difference in the number of atoms N_2 in $|2\rangle$ between these two measurements:

$$S = N \sin\left(\frac{A_{\rm PC}t_c}{\hbar}\right)\sin\left(\frac{A_{\rm PNC}t_c}{\hbar}\right) \approx N \sin\left(\frac{A_{\rm PC}t_c}{\hbar}\right)\frac{A_{\rm PNC}t_c}{\hbar}. \quad (5)$$

Figure 1 shows the principle of the measurement. We plot the evolution of the population in the upper hyperfine state $|2\rangle$ as a function of time (Eq. 4), as

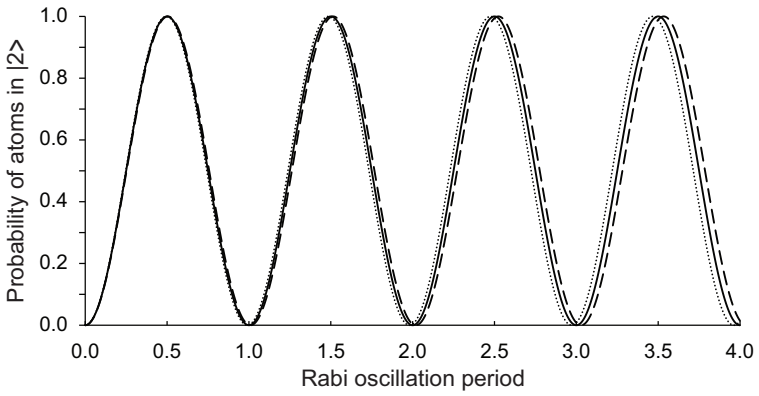

Fig. 1 Probability of finding the atoms in the upper hyperfine state ($|2\rangle$) as a function of time with (dotted and dashed lines for each apparatus handedness) and without (continuous line) the presence of the *nsd*-APNC weak interaction. The strength of the APNC effect has been exaggerated for figure clarity.

it undergoes Rabi oscillations. The continuous line represents the oscillation in the absence of the weak interaction. For the purposes of illustration we exaggerate many orders of magnitude the size of the weak interaction and plot the evolution with both possible handednesses (dotted and dashed lines). We extract the signal S (Eq. 5) from the difference between the dashed and the dotted lines at a given time (in multiples or fractions of a period of the Rabi oscillation). Ref. [40] describes in detail our successful test of this scheme to recover a very small artificial coherent signal with Rb atoms in an optical blue-detuned dipole trap. The continual application of both the $A_{\rm PNC}$ and $A_{\rm PC}$ driving fields throughout the Rabi process poses extra constraints on the performance of the trap and apparatus in general [38,41,42].

The measurement will proceed as follows: We trap and cool atoms on-line at the ISAC facility at TRIUMF using our high efficiency magneto optical trap (MOT) [43]. The cold francium sample is then transferred to a science chamber with precision control of all electric, magnetic, and electromagnetic fields, as well as superior vacuum.

The atoms in the science chamber will be held in a blue detuned dipole trap [41], which is at the electric field antinode of a microwave Fabry-Perot cavity tuned to the hyperfine splitting [38]. Simultaneously, we will apply a parity-conserving magnetically driven $M1$ interaction to interfere with the parity-violating $E1$ transition driven by the cavity microwave electric field. The time to measure the difference between the two populations is determined by $A_{\rm PC}t_c/\hbar = (n/2 + 1/4)\pi$. This makes the measurement most sensitive (linear section of the oscillation) to the change due to the interference with the *nsd*-PNC signal. The specific choice of n Rabi oscillations depends on the coherence time of the sample t_c, but we have reached more than 100 ms in tests with Rb [40]. To illustrate the expected numbers, we consider

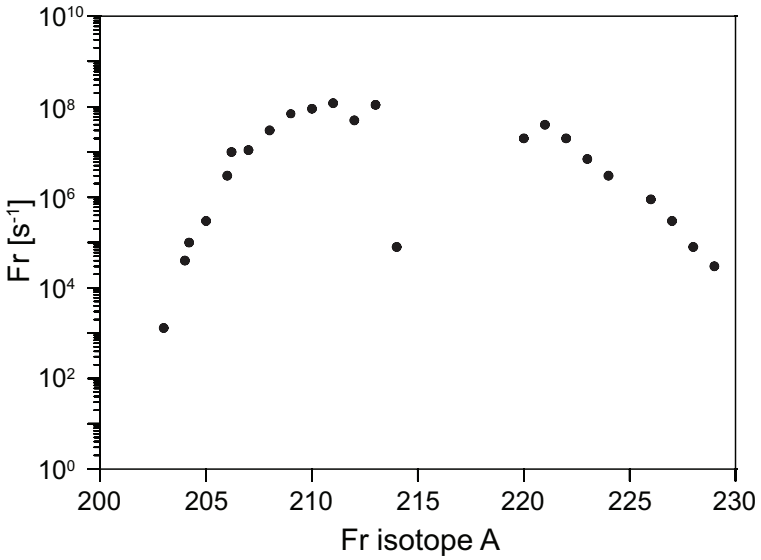

Fig. 2 Production yield of Fr isotopes at the ISAC facility in TRIUMF with a UC target in December 2010.

the case of ^{209}Fr: if we have a field of 476 V/cm to drive the $E1$ transition and a coherent interaction time of 100 ms, then $|A_{\rm PNC}/\hbar| = 0.01$ rad/s and $A_{\rm PC}/\hbar = (2n+1) \times 7.85$ rad/s [38].

The signal to noise ratio (S/N) in the projection noise limited measurement [44] is:

$$\frac{S}{N} = 2\frac{A_{\rm PNC} t_c}{\hbar}\sqrt{N}, \tag{6}$$

where the success of the experiment relies on the number of atoms, long coherence time and high intensity of the microwave field.

For an optical dipole trap population of N =10^6 Fr atoms, the expected signal-to-noise ratio is $S/N = 2$ per measurement. After each measurement, the Fr are optically pumped back into the start hyperfine state $\langle 1|$, and the measurement processed is repeated. The expected measurement cycle is expected to have a period on the order of 1 s. The francium sample will be depleted by the imperfect vacuum of the science chamber and so will need of replenished from the capture MOT every 20 s or so.

3 Current Status of the Experiment at TRIUMF

Reference [13] summarizes our work at the Stony Brook linear accelerator (LINAC) where we first produced and laser-trapped francium. This first set of Fr experiments was used to study many of the relevant atomic and nuclear properties necessary for future APNC measurements. Since the closing of the

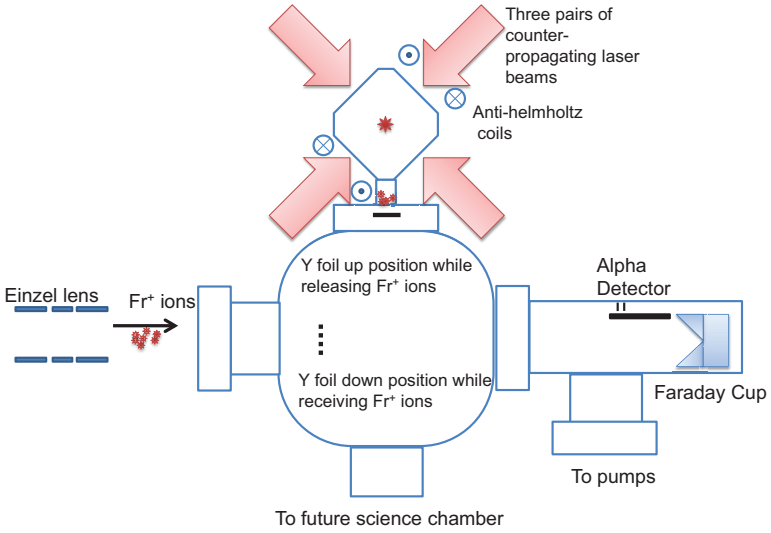

Fig. 3 (Color on-line) Schematic of the capture chamber for Fr isotopes at the ISAC facility in TRIUMF.

Stony Brook LINAC we have continued the construction and development of the apparatus at the University of Maryland. We moved the apparatus to the ISAC hall at TRIUMF in Vancouver in the fall of 2011, where we now have the system ready for commissioning runs during the fall of 2012.

The ISAC facility at TRIUMF, using 2 μA of 500 MeV on an actinide target of UC_x (30g/cm^2), has been able to produce the yields shown in Fig. 2 in Dec. 2010. We expect similar performance in the near future and we are particularly encouraged by the yields around 211, near the closed neutron shell. The yield is two orders of magnitude larger than ever achieved at Stony Brook with a fusion evaporation reaction of O on Au at around 100 MeV [45].

3.1 The capture chamber

Figure 3 shows a schematic of the capture chamber and trap currently at TRIUMF. The setup is based on the one at Stony Brook [43] that relies on capturing the activity in a Y neutralizer for a period of time and then releasing the activity into a closed glass cell for the trapping. The chamber is made mostly of stainless steel commercial parts with minimal modifications to ensure smooth rotation of the moving neutralizer parts. The Fr beam first encounters a collimating aperture (8.5 mm diameter) that can be used for tuning the ion beam.The aperture is not shown in the drawing. All the parts related to the Y neutralizer are mounted on a 4.5-inch conflat flange. This arrangement ensures reliable alignment and facilitates the electrical connections that must be made and tested before the system is closed. Fig 3 shows the direction of the ion

beam entrance towards the Y holder in the catching position (dashed). It has a movable neutralizer holder that rotates off-axis. The continuous line shows the neutralizer in its delivery position when a current runs through the thin foil raising its temperature to about 1000 K. The chamber has viewing ports that allow observation of the neutralizer holder to measure the temperature and ensure its proper rotation. There is a nipple with Rb dispensers, not shown in the schematic, for tests with stable atoms. Two pumps maintain the vacuum in the chamber. A conical Faraday cup sits in-line with the Fr^+ beam in an appendix on the vacuum port behind the neutralizer holder to monitor the current. An off-axis silicon detector next to the Faraday cup can measure alpha activity of the decaying Fr nuclei.

The figure also shows the MOT glass cell mounted on top of the neutralizer chamber surrounded by the optics that deliver the laser beams on each side of the glass cell cube. Three identical sets of optics expand optical-fiber delivered beams into 5 cm diameter beams. The beams are collimated and circularly polarized. A further three sets of optics retro-reflect the laser light while keeping the helicity of the light the same as the incident beam.

Two CCD cameras and a photomultiplier tube with a 1:1 imaging system image the trap. This imaging system is attached to a photomultiplier tube capable of photon counting for spectroscopy of trapped Fr atoms. The cooling, trapping, and spectroscopy probe lasers reside on a separate optical table in the laboratory and are all locked and controlled using a single scanning Fabry-Perot cavity [46]. The titanium-sapphire and diode lasers cover the necessary wavelengths for Rb (780 nm, 795 nm) and Fr (718 nm and 817 nm) trapping. The polarization elements at the trap are optimized for 718 nm. Water cooled coils provide a magnetic field gradient of 7 G/cm (strong axis) for operation of the MOT, but are capable of up to 20 G/cm. Not shown in Fig. 3 are six extra coils that can be used to compensate environmental magnetic fields.

3.2 The science chamber

The science chamber has been thoroughly tested at the University of Maryland before the move to TRIUMF. It is a large vacuum vessel with differential pumping and numerous windows and access ports. The development of the optical dipole trap and its characterization with Rb has shown that we can reach the sensitivity for the anapole measurement [40–42]. We are pursuing quasi-optic approaches for the microwave cavity and reached Q factors at the necessary frequencies of 46 GHz in excess of 3×10^4. There remain many other experimental issues to control, but we can see a clear path for future experiments that measure the weak interaction through PNC in atoms. Refs. [38, 41] present careful analysis of possible systematic effects in the anapole measurement and how to prevent and diagnose them.

After the initial commissioning run and preliminary spectroscopic measurements, we will connect the science chamber to the capture chamber for the studies of weak interaction physics in neutral Fr.

4 Acknowledgments

We would like to thank the ISAC staff at TRIUMF for developing the Fr beam. Our work is supported by NRC, TRIUMF, and NSERC from Canada, DOE, and NSF from the USA, and CONACYT from Mexico.

References

1. M.A. Bouchiat, C. Bouchiat, Rep. Prog. Phys. **60**, 1351 (1997)
2. G. Gwinner, E. Gomez, A. Pérez Galván, D. Sheng, Y. Zhao, L.A. Orozco, G.D. Sprouse, J.A. Behr, K.P. Jackson, M.R. Pearson, V. Flambaum, S. Aubin, Hyp. Int. **172**, 45 (2006)
3. Y.B. Zel'dovich, Sov. Phys. JETP **9**, 682 (1959)
4. V.V. Flambaum, I.B. Khriplovich, O.P. Sushkov, Phys. Lett. B **146**, 367 (1984)
5. V.V. Flambaum, D.W. Murray, Phys. Rev. C **56**, 1641 (1997)
6. W.C. Haxton, C.E. Wieman, Annu. Rev. Nucl. Part. Sci. **51**, 261 (2001)
7. W.R. Johnson, M.S. Safronova, U.I. Safronova, Phys. Rev. A **67**, 062106 (2003)
8. J.S.M. Ginges, V.V. Flambaum, Phys. Rep. **397**, 63 (2004)
9. M.A. Bouchiat, C. Bouchiat, J. Phys. (Paris) **35**, 899 (1974)
10. M.A. Bouchiat, C. Bouchiat, Phys. Lett. B **48**, 111 (1974)
11. M.A. Bouchiat, C. Bouchiat, J. Phys. (Paris) **36**, 493 (1975)
12. W.J. Marciano, J.L. Rosner, Phys. Rev. Lett. **65**, 2963 (1990)
13. E. Gomez, L.A. Orozco, G.D. Sprouse, Rep. Prog. Phys. **66**, 79 (2006)
14. J.A. Behr, G. Gwinner, J. Phys G; Nucl. and Prt. Phys. **36**, 033101 (2009)
15. H. Davoudiasl, H.S. Lee, W.J. Marciano, Phys. Rev. Lett. **109**, 031802 (2012). DOI 10.1103/PhysRevLett.109.031802
16. V.A. Dzuba, V.V. Flambaum, O.P. Sushkov, Phys. Rev. A **51**, 3454 (1995)
17. M.S. Safronova, W.R. Johnson, Phys. Rev. A **62**, 022112 (2000)
18. M.A. Bouchiat, C. Bouchiat, Eur. Phys. J. D **15**, 5 (2001)
19. M.J.D. Macpherson, K.P. Zetie, R.B. Warrington, D.N. Stacey, J.P. Hoare, Phys. Rev. Lett. **67**, 2784 (1991)
20. D.M. Meekhof, P. Vetter, P.K. Majumder, S.K. Lamoreaux, E.N. Fortson, Phys. Rev. Lett. **71**, 3442 (1993)
21. D.M. Meekhof, P. Vetter, P.K. Majumder, S.K. Lamoreaux, E.N. Fortson, Phys. Rev. A **52**, 1895 (1995)
22. P.A. Vetter, D.M. Meekhof, P.K. Majumder, S.K. Lamoreaux, E.N. Fortson, Phys. Rev. Lett. **74**, 2658 (1995)
23. C.S. Wood, S.C. Bennett, D. Cho, B.P. Masterson, J.L. Roberts, C.E. Tanner, C.E. Wieman, Science **275**, 1759 (1997)
24. C.S. Wood, S.C. Bennett, J.L. Roberts, D. Cho, C.E. Wieman, Can. J. Phys. **77**, 7 (1999)
25. J. Guéna, D. Chauvat, P. Jacquier, E. Jahier, M. Lintz, S. Sanguinetti, A. Wasan, M.A. Bouchiat, A.V. Papoyan, D. Sarkisyan, Phys. Rev. Lett. **90**, 143001 (2003)
26. D. DeMille, Phys. Rev. Lett. **74**, 4165 (1995)
27. J.E. Stalnaker, D. Budker, D.P. DeMille, S.J. Freedman, V.V. Yashchuk, Phys. Rev. A **66**, 031403 (2002)
28. K. Tsigutkin, D. Dounas-Frazer, A. Family, J.E. Stalnaker, V.V. Yashchuk, D. Budker, Phys. Rev. Lett. **103**, 071601 (2009)
29. K. Tsigutkin, D. Dounas-Frazer, A. Family, J.E. Stalnaker, V.V. Yashchuk, D. Budker, Phys. Rev. A **81**, 032114 (2010)
30. D.R. Dounas-Frazer, K. Tsigutkin, D. English, D. Budker, Phys. Rev. A **84**, 023404 (2011)
31. D. Budker, D. DeMille, E.D. Commins, M.S. Zoltorev, Phys. Rev. Lett. **70**, 3019 (1994)
32. A.T. Nguyen, D. Budker, D. DeMille, M. Zolotorev, Phys. Rev. A **56**, 3453 (1997)
33. E.N. Fortson, Phys. Rev. Lett. **70**, 2383 (1993)

34. T.W. Koerber, M. Schacht, W. Nagourney, E.N. Fortson, J. Phys. B **36**, 637 (2003)
35. A. Kleczewski, M.R. Hoffman, J.A. Sherman, E. Magnuson, B.B. Blinov, E.N. Fortson, Phys. Rev. A **85**, 043418 (2012)
36. O.O. Versolato, L.W. Wansbeek, G.S. Giri, J.E. van den Berg, D.J. van der Hoek, K. Jungmann, W.L. Kruithof, C.J. Onderwater, B.K. Sahoo, B. Santra, P.D. Shidling, R.G. Timmermans, L. Willmann, H.W. Wilschut, Canadian Journal of Physics **89**, 65 (2011)
37. D. DeMille, S.B. Cahn, D. Murphree, D.A. Rahmlow, M.G. Kozlov, Phys. Rev. Lett. **100**, 023003 (2008)
38. E. Gomez, S. Aubin, G.D. Sprouse, L.A. Orozco, D.P. DeMille, Phys. Rev. A **75**, 033418 (2007)
39. A. Corney, *Atomic and Laser Spectroscopy* (Clarendon Press, Oxford, 1977)
40. D. Sheng, J. Zhang, L.A. Orozco, Rev. Sci. Instr. **83**, 043106 (2012)
41. D. Sheng, L.A. Orozco, E. Gomez, J. Phys. B **43**, 074004 (2010)
42. D. Sheng, J. Zhang and L. A. Orozco, in preparation.
43. S. Aubin, E. Gomez, L.A. Orozco, G.D. Sprouse, Rev. Sci. Instrum. **74**, 4342 (2003)
44. W.M. Itano, J.C. Begquist, J.J. Bollinger, J.M. Gilligan, D.J. Heinzen, F.L. Moore, M.G. Raizen, D.J. Wineland, Phys. Rev. A **47**, 3554 (1993)
45. J.E. Simsarian, A. Ghosh, G. Gwinner, L.A. Orozco, G.D. Sprouse, P.A. Voytas, Phys. Rev. Lett. **76**, 3522 (1996)
46. W.Z. Zhao, J.E. Simsarian, L.A. Orozco, G.D. Sprouse. Rev. Sci. Instrum. **69**, 3737 (1998)